A new series of fluorescent 5-methoxy-2-pyridylthiazoles with a pH-sensitive dual-emission†

Ming-Hua Zheng,[ab] Jing-Yi Jin,[ab] Wei Sun[a] and Chun-Hua Yan*[a]

Received (in Montpellier, France) 4th April 2006, Accepted 19th May 2006
First published as an Advance Article on the web 14th June 2006
DOI: 10.1039/b604910a

A new series of fluorophores, 5-methoxy-2-(2-, 3- or 4-pyridyl)thiazoles (2-, 3- or 4-MPT, respectively), were synthesized and their photophysical properties investigated. 2- and 4-MPT are highly fluorescent in polar solvents. Combined with theoretical calculations, studies of the excited state lifetimes in different solvents reveal that their fluorescence mainly results from the internal charge transfer excited state. Acidobasic properties of their ground states and excited states were studied with steady and transient fluorescence spectroscopy. 2- and 4-MPT displayed a pH sensitive fluorescent behavior with a dual-emission in the range 2 to 6 in an aqueous system.

Introduction

Optical pH sensors have been extensively applied in analytical chemistry, biochemistry, cellular biology and medicine.[1] In particular, pH sensors based on the change of fluorescence exhibit a lot of advantages such as high sensitivity and ease of miniaturization.[2] For the practical measurement of pH, a ratiometric fluorescent pH sensor with a dual-emission is more attractive due to its insensitivity to sample orientation, probe concentration, photobleaching and background fluorescence.[3] Many efforts have been made to develop a ratiometric fluorescent pH sensor in various ranges to meet different demands.[4,5]

However, the design of a pH-sensitive fluorophore with a dual-emission is delicate. There are still challenges from the viewpoints of both synthesis and quantum yield.[5a] Recently Jullien and co-workers reported a new series of fluorescent 5-aryl-2-pyridyloxazoles (PYMPO) as ratiometric fluorescent pH sensors with a dual-emission.[5b] In fact, 1,3-thiazole can act as a spacer between the electron donor and acceptor as a structural analog of 1,3-oxazole,[6] which has been previously demonstrated in Thiazole Orange (TO) as a fluorescent label for biological systems in 1986.[7] In the present work, we report the synthesis and optical properties of a new series of fluorophores, 5-methoxy-2-(2-, 3- or 4-pyridyl)thiazoles (2-, 3- or 4-MPT, respectively). The fluorescence quantum yields of the 2- and 4-substituted isomers (2- and 4-MPT) are high in polar solvents. Studies of both the steady and transient fluorescence spectra disclose that an internal charge transfer (ICT) excited state is evolved upon excitation, which is supported by theoretical calculations. The acidobasic properties of the MPTs in both the ground and the excited states were investigated. 2- and 4-MPT displayed a ratiometric pH-sensitive fluorescence behavior with a dual-emission.

Results and discussion

Synthesis

Reaction of pyridyl carboxylic acid chloride and glycine methyl ester hydrochloride in the presence of triethylamine (TEA), and subsequently followed by a reaction with Lawesson's reagent[8] resulted in the formation of the MPTs (Scheme 1).

Optical properties

The absorption and fluorescence maxima of the MPTs are collected in Table 1. All MPTs are fluorescent, and especially the fluorescence quantum yields of 2- and 4-MPT are very high and comparable to a reported series of 1,3-oxazole derivatives.[5b] The fluorescence intensity of the MPTs increased proportionally to their concentration between 10^{-7} to 10^{-5} M, thus the emission is attributed to the monomeric species but not the dimer or excimer (see Fig. S10 in ESI†).

A typical charge transfer process in MPTs can be concluded experimentally. A bathochromic shift of the fluorescence emission of the MPTs was observed as the polarity of the solvents increased. According to a theoretical model of the photoinduced charge transfer for the push–pull conjugated molecules,[12] increasing the polarity of the solvent has no significant effect on the wavelength of absorption whereas it

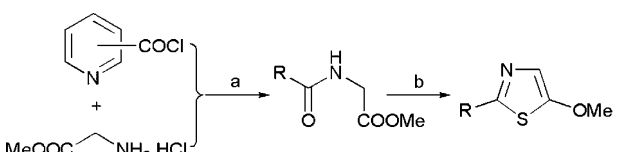

R = 2-pyridyl: **2-MPT** (53 %);
3-pyridyl: **3-MPT** (58 %);
4-pyridyl: **4-MPT** (50 %).

a. TEA, 0 °C; b. Lawesson's reagent, $PhCH_3$, reflux.

Scheme 1 Synthesis of 5-methoxy-2-pyridylthiazole.

[a] *Beijing National Laboratory for Molecular Sciences, State Key Lab of Rare Earth Materials Chemistry and Applications & PKU-HKU Joint Lab in Rare Earth Materials and Bioinorganic Chemistry, Peking University, Beijing 100871, China*
[b] *Department of Chemistry, Yanbian University, Yanji, Jilin 133002, China*

† Electronic supplementary information (ESI) available: Absorption and excitation spectra, steady fluorescence spectra of MPTs and fluorescence decay curves of 2- and 4-MPTs at different pH. See DOI: 10.1039/b604910a

Table 1 Photophysical properties of MPTs. Maxima[a] of absorption λ_{abs} and of steady fluorescence emission[b] λ_{em}, molar absorption coefficients $\varepsilon_{max} \pm 5\%$, fluorescence quantum yields[c] $\Phi \pm 5\%$, the Stokes shifts ΔS and the lifetime[d] of the excited states τ in different solvents

	Solvent (Δf)[e]	*n*-Hexane (0.0002)	Chloroform (0.149)	Tetrahydrofuran (0.210)	Dichloromethane (0.219)	Acetonitrile (0.306)	Methanol (0.309)	Water[f] (0.320)
2-MPT	λ_{abs}/nm	320	322	323	321	320	321	323
	log (ε_{max}/M^{-1} cm^{-1})	4.20	4.30	4.34	4.21	3.92	3.93	4.21
	λ_{em}/nm	384	390	392	391	397	397	403
	Φ	0.73	0.91	0.90	0.94	0.88	0.94	0.74
	ΔS/cm^{-1}	5208	5415	5450	5577	6061	5963	6146
	τ/ns	2.5	2.8	2.8	2.9	3.2	3.2	3.6
4-MPT	λ_{abs}/nm	312	320	319	317	318	322	322
	log (ε_{max}/M^{-1} cm^{-1})	3.98	3.70	4.06	3.93	3.70	3.64	3.99
	λ_{em}/nm	371	385	388	385	391	404	406
	Φ	0.12	0.67	0.48	0.59	0.59	0.56	0.43
	ΔS/cm^{-1}	5097	5276	5575	5572	5871	6303	6425
	τ/ns	—[g]	1.2	1.3	1.4	2.5	4.7	2.3
3-MPT	λ_{abs}/nm	309	314	313	313	311	313	312
	log (ε_{max}/M^{-1} cm^{-1})	4.22	4.18	4.28	4.01	3.98	3.89	4.29
	λ_{em}/nm	367	378	379	381	388	396	406
	Φ	0.10	0.31	0.25	0.36	0.2	0.26	0.16
	ΔS/cm^{-1}	5115	5392	5564	5702	6381	6696	7421
	τ/ns	—[g]	—[g]	—[g]	1.2	—[g]	—[g]	—[g]

[a] All spectra were recorded at 293 K. General concentrations of analysts were 25 and 1 μM, respectively, for measurement of absorption and steady fluorescence emission. [b] Excited at 310, 320 and 310 nm for 2-MPT, 4-MPT and 3-MPT, respectively. [c] Relative quantum yields were evaluated using quinine sulfate ($\Phi = 0.48 \pm 0.2$) in 0.5 M H_2SO_4, excited at 313 nm) as the standard compound.[9] [d] Lifetimes of the excited state of 2-MPT were fitted monoexponentially, and lifetimes of the excited states of 4-MPT and 3-MPT were fitted double-exponentially and calculated with the corresponding weights.[10] [e] Δf was the orientation polarizability (Lippert's solvent polarity parameter),[4a,11] which was used to correlate the Stokes shifts and the polarities of solvents. [f] The aqueous solutions were prepared using twice distilled water. [g] Difficult to obtain accurate data because of the low fluorescence quantum yields.

promotes a red shift in the emission, resulting in an increasing Stokes shift of the MPTs with the polarity of solvent as listed in Table 1.

Studies of the fluorescence decays of the MPTs reveal that the lifetimes of the fluorescent excited state of MPTs were also affected by the polarity of the solvents (Table 1).

Theoretical calculations

Density functional calculations of MPTs were performed at the B3LYP/6-31G(d,p) level using Gaussian 03.[13] Geometry optimization produced similar coplanar structures for all MPTs (see Fig. S17 in ESI†). The electron density is mainly located at the methoxy group and the thiazole ring in the HOMO (Fig. 1), while in the LUMO, the electron density is located at the pyridyl ring. Based on experimental and theoretical results, it can be deduced that the ICT excited states of MPTs are evolved upon excitation and photoinduced charge transfer occurs from the electron donating 5-methoxy group to the 2-pyridyl ring.

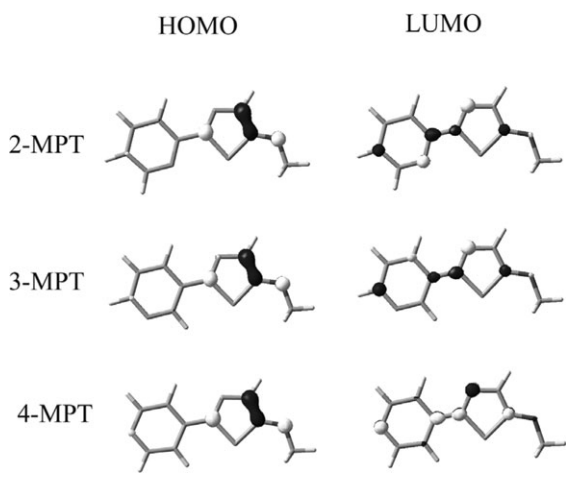

Fig. 1 HOMO and LUMO of MPTs at the B3LYP/6-31G(d,p) level of theory calculated by Gaussian 03.

Acidobasic properties of the ground and excited states

Both the maxima of the absorption and the fluorescence of MPTs were red shifted with the decrease in pH. The typical evolution of the pH-dependent absorption and emission of MPTs is illustrated in Fig. 2.

Such bathochromic absorption and emission are assigned to the protonated form, MPT–H$^+$. Theoretically, protonation occurs at the nitrogen atom of the pyridyl ring, giving rise to an acidic MPT–H$^+$. Compared with the parent MPT, protonation decreases the energy difference between the HOMO and LUMO[5b] in the protonated MPT–H$^+$ and thus favors charge transfer from the methoxy group to the pyridyl ring through the thiazole ring. The photophysical data of the protonated form of the MPTs are collected in Table 2.

A clear and fixed isosbestic point is observed in the evolution of both the UV-Vis absorption and fluorescence emission spectra at different pH for every MPT, which indicated the presence of an equilibrium of protonation between the acidic and basic forms of MPTs in solution (Scheme 2).

The pK_a (MPT–H$^+$/MPT) value of the ground states of MPTs were then calculated from the UV-Vis absorption titration experiments. For the excited states of MPTs, an increased pK_a* ([MPT–H$^+$]*/[MPT]*) could be anticipated

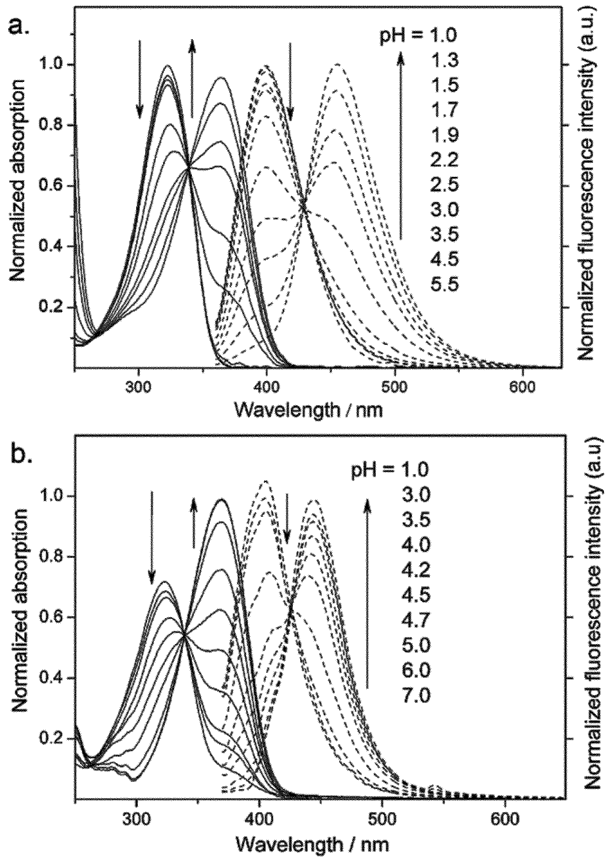

Fig. 2 Evolution of absorption and fluorescence emission of (a) 2-MPT excited at 350 nm and (b) 4-MPT excited at 355 nm with pH in an aqueous system at 293 K. Solid line: absorption; dashed line: fluorescence.

because the photoinduced charge transfer results in a larger population of electrons at the pyridine ring. According to the Förster cycle, we evaluated the pK_a* values from eqn. (1):[4a]

$$2.3RT(\mathrm{p}K_a^{*} - \mathrm{p}K_a) = N_a[h\nu(\mathrm{MPT}) - h\nu(\mathrm{MPT\text{–}H^+})] \quad (1)$$

where the ionization entropies ΔS^0 and ΔS^{0}* of MPT–H^+ and (MPT–H^+)*, respectively, are reasonably assumed to be equal, R is the gas constant, T is the absolute temperature, ν(MPT) and ν(MPT–H^+) are the energy differences (corresponding to the 0–0 transitions) between the excited state and the ground state of MPT and MPT–H^+, respectively, and N_a is Avogadro's number. After converting the frequency (ν^{-1}) into the wavenumber (cm^{-1}) and estimating the 0–0 transitions of MPT and MPT–H^+ by means of the wavenumber average (eqn. (2)) between the corresponding maxima of absorption and emission, eqn. (3)[14] is obtained.

$$\nu_{0\text{–}0}{}^{-1} = (\nu_{abs}{}^{-1} + \nu_{em}{}^{-1})/2 \quad (2)$$

$$\mathrm{p}K_a^{*} - \mathrm{p}K_a = 2.1\times10^{-3}[\nu_{abs}(\mathrm{MPT})^{-1} + \nu_{em}(\mathrm{MPT})^{-1} - \nu_{abs}(\mathrm{MPT\text{–}H^+})^{-1} - \nu_{em}(\mathrm{MPT\text{–}H^+})^{-1}] \quad (3)$$

From the estimated pK_a* values (Table 2), the excited state of MPT is significantly more basic compared with the corresponding MPT ground state, indicating that photoinduced charge transfer occurred upon excitation of the MPTs.

Table 2 Photophysical data of the protonated MPTs. Maxima[a] of absorption λ_{abs} and of steady fluorescence emission[b] λ_{em}, molar absorption coefficients ε_{max} ± 5%, fluorescence quantum yields[c] Φ ± 5%, lifetimes[d] of the excited states τ at pH = 1.0, pK_a and pK_a* of the ground states[e] and excited states, respectively, in an aqueous system at 293 K

	2-MPT–H^+	4-MPT–H^+	3-MPT–H^+
λ_{abs}/nm	364	369	331
log (ε_{max}/M^{-1} cm^{-1})	4.25	4.05	4.10
λ_{em}/nm	455	445	514
Φ	0.76	0.47	0.01
τ/ns	3.7	9.4	—[f]
pK_a ± 0.1	1.6	4.3	3.3
pK_a*	8.2	12.4	11.2

[a] All spectra measurements were taken at 293 K. General concentrations of analysts were 25 μM and 1 μM, respectively, for measurement of absorption and steady fluorescent emission. [b] Excited at 360, 360 and 330 nm for 2-MPT, 4-MPT and 3-MPT, respectively, at pH = 1.0. [c] Relative quantum yields were evaluated using quinine sulfate (Φ = 0.48 ± 0.2) in 0.5 M H_2SO_4 (excited at 313 nm) as the standard compound.[12] [d] Lifetimes of the excited state of 2-MPT were fitted monoexponentially, and 4-MPT and 3-MPT were fitted double-exponentially, and calculated according to the lifetimes and the corresponding weights.[10] [e] pK_a values of the ground state were evaluated from UV titration experiments. [f] Difficult to obtain accurate data because of the low fluorescence quantum yields of 3-MPT.

Mechanism of pH sensing

Due to the dual-emission and the high fluorescence quantum yields of MPTs, 2- and 4-MPT may be expected to be applied in a ratiometric fluorescent pH sensor. Although they are structural analogs of PYMPO, the protonation–deprotonation processes of the excited state were somewhat different according to studies of the fluorescence decay of 2- and 4-MPT in the measured pH ranges. The lifetimes of both (2-MPT)* and (2-MPT–H^+)* were fitted monoexponentially (Table 3). At pH < 3.0, the extracted lifetimes of the fluorescent excited states (λ_{em} = 400 nm excited at 310 nm) dropped as pH was lowered, attributed to a dynamic quenching by the proton according to the Stern–Volmer analysis (Fig. 3).[4a] The fitted $k_Q = 0.5 \times 10^{10}$ M^{-1} s^{-1} indicated that the dynamic quenching of the fluorescence of 2-MPT by the proton was diffusion-controlled.[5b] Meanwhile, the lifetime of the excited state of 2-MPT–H^+ (λ_{em} = 455 nm excited at 365 nm) did not change at pH below 3.0, indicating a stable fluorescence (2-MPT–H^+)*. Based on the extracted lifetimes of (2-MPT)* and (2-MPT–H^+)*, 3.4 and 3.8 ns, respectively, it is postulated that the protonation of 2-MPT*

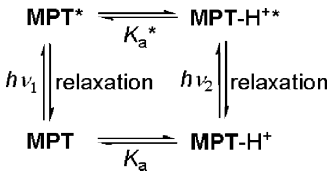

Scheme 2 Schematic representation of the protonation equilibria of the ground and excited states of MPTs.

Table 3 Lifetimes τ of 2-MPT and 4-MPT at different pH[a]

	2-MPT				4-MPT					
	λ_{em} = 400 nm (λ_{ex} = 310 nm)		λ_{em} = 455 nm (λ_{ex} = 365 nm)		λ_{em} = 400 nm (λ_{ex} = 320 nm)			λ_{em} = 445 nm (λ_{ex} = 365 nm)		
pH	$\tau \pm 0.1$/ns	χ^2	$\tau \pm 0.1$/ns	χ^2	$\tau_1 \pm 0.1$/ns	$\tau_2 \pm 0.1$/ns	χ^2	$\tau_1' \pm 0.1$/ns	$\tau_2' \pm 0.1$/ns	χ^2
1.0	1.2	1.017	3.8	1.019	—[c]			0.3 (76.14)	10.4 (23.86)	1.029
1.5	2.2	1.057	3.8	1.019	2.1 (13.43)	12.8 (86.57)	1.052	0.3 (77.97)	10.0 (22.03)	1.043
2.0	2.9	1.051	3.8	1.006	2.1 (29.32)	12.5 (70.68)	1.013	0.3 (77.67)	10.3 (22.33)	1.025
2.5	3.3	1.003	3.8	1.012	2.1 (57.85)	12.1 (42.15)	1.024	0.3 (71.79)	10.8 (28.21)	1.034
3.0	3.4	1.039	—[b]		2.1 (77.53)	11.9 (22.47)	1.007	0.3 (70.36)	10.2 (29.64)	1.020
3.5	3.4	1.009			2.1 (91.40)	9.5 (18.60)	1.071		—[b]	
4.0	3.4	1.054			2.1 (91.20)	9.0 (8.80)	1.005			
4.5	3.4	1.015			2.1 (90.34)	8.4 (9.66)	1.008			
5.0	3.4	1.065			2.1 (90.48)	8.4 (9.52)	1.071			
5.5	3.4	1.060			2.1 (90.73)	9.0 (9.27)	1.010			
6.0	3.4	1.054			2.1 (89.91)	8.6 (10.09)	0.943			

[a] Determined at 293 K. [b] Difficult to obtain accurate data due to the weak fluorescence under the measurement conditions. [c] Not determined.

resulted in the generation of (2-MPT–H^+)* and the subsequent deprotonation of (2-MPT–H^+)* should not occur in the excited state.

The double-exponentially fitted lifetime of the excited states of 4-MPT implied that there are two components responsible for the fluorescence, which leads to a different pH sensing mechanism from 2-MPT. We assign component 1 of 4-MPT* (λ_{em} = 400 nm, excited at 320 nm) as the main fluorescent species because the percentage of component 1 decreased as the pH value dropped (Table 3), which is consistent with the evolution of the steady fluorescences. The lifetime of component 1 is almost constant in pH 6.0–1.5. Regarding the proton as the quencher of the fluorescence of 4-MPT (λ_{em} = 400 nm, excited at 320 nm), formation of a stable complex 4-MPT–H^+ in the ground state is responsible for the observed static quenching. Meanwhile, the lifetime of component 1′ of (4-MPT–H^+)* is unvaried as 0.3 ns at pH < 3, similar to the case of (2-MPT–H^+)*. Therefore, the fluorescent excited state of (4-MPT–H^+)* mainly originates from the excitation of the protonated 4-MPT, and the possibility of deprotonation in the excited state might be low.

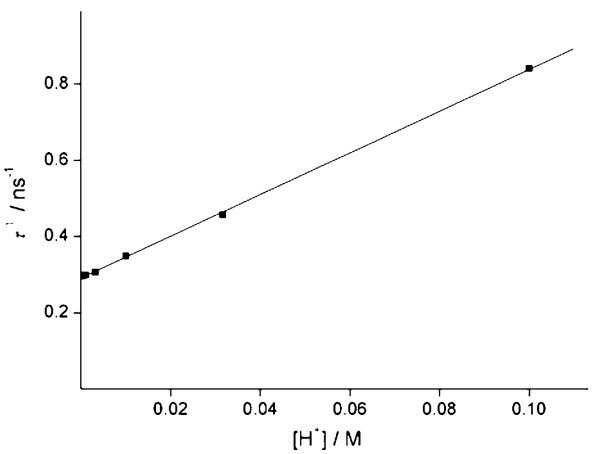

Fig. 3 Stern–Volmer analysis of the lifetimes of the excited state of 2-MPT below pH 3.0.

Conclusions

In the present work, we successfully developed a new series of fluorophores with synthetic simplicity and high fluorescence quantum yields. The internal charge transfer excited states are evolved upon excitation, and have been investigated and analysed according to both experimental results and theoretical calculations. Although different kinetics influenced the protonation processes of 2- and 4-MPT in the ground and excited states, both of them displayed a pH-sensitive fluorescence behavior with a dual-emission.

Experimental

Materials and methods

All reactions were performed under argon atmosphere using purified solvents by standard methods. All chemicals were purchased from Acros and used as received without further purification. For all spectrometric measurements, HPLC grade solvents were degassed before use. For chromatography, 100–200 mesh silica gel (Qingdao, China) was used.

The UV-Vis absorption spectra were measured with a Hitachi U-3010 spectrophotometer and the fluorescence spectra were recorded on a Hitachi F-4500 fluorescence spectrophotometer. Time-resolved fluorescence spectra were obtained using an Edinburgh FLS920 fluorescence spectrophotometer. The instrument was operated with a thyratron-gated flash lamp filled with hydrogen at a pressure of 0.5 atm. The lamp was operated at a frequency of 40 kHz and the pulse width of the lamp under operating conditions was about 1.2 ns. The lifetimes were estimated from the measured fluorescence decay curves and the lamp profile using a nonlinear least squares iterative fitting procedure. NMR spectra were recorded on a Varian Mercury 200 spectrometer. Chemical shifts were reported in ppm using tetramethylsilane (TMS) as the internal standard. IR spectra were recorded on a Nicolet 5MX-S infrared spectrometer. Elemental analyses (C, H, N) were performed on an Elementar Vario EL analyzer.

All spectra measurements were recorded at 20 °C. Unless mentioned otherwise, concentrations of analysts were 25 μM

and 1 μM, respectively, for measurement of UV-Vis absorption and fluorescence emission spectra. The pH values were adjusted by addition of 0.1 M HCl and then determined by a pH-meter at 20 °C.

Syntheses

5-Methoxy-2-(2-pyridyl)thiazole (2-MPT). Picolinoyl chloride hydrochloride (780 mg, 4.38 mmol) was dissolved in 5 mL dried chloroform, then added slowly into a chloroform solution (10 mL) containing glycine methyl ester hydrochloride (550 mg, 4.38 mmol) and triethylamine (1.3 mL, 11 mmol) at 0 °C. After stirring for 2 h, the solvent was removed under reduced pressure. The resulting mixture was partitioned by water, extracted with ethyl acetate (3 × 80 mL) and dried over Na_2SO_4. The organic phase was condensed under reduced pressure, and recrystallization from *n*-hexane and ethyl acetate provided the desired amide as a white solid (731 mg, yield: 86%).

The obtained amide (1.0 g, 5.15 mmol) and Lawesson's reagent (2.5 g, 6.18 mmol) were refluxed in dried toluene for 20 h under Ar atmosphere. The resulting slurry was poured into a 10 M NaOH aqueous solution in an ice bath and extracted with ethyl acetate. The organic layer was evaporated under reduced pressure after being dried over Na_2SO_4. The obtained oil was subjected to chromatography on silica gel using CH_2Cl_2 and ethyl acetate as eluent, and after recrystallization from *n*-hexane and ethyl acetate 5-methoxy-2-(2-pyridyl)thiazole was obtained as a white solid (525 mg, yield: 53%).

Mp: 46–47 °C. IR (KBr, cm^{-1}): 1531, 1490, 1455, 1439, 1419, 1252, 998, 779. ^1H NMR ($CDCl_3$, 200 MHz): δ = 8.55–8.51 (m, 1H), 8.07–8.02 (m, 1H), 7.78–7.69 (m, 1H), 7.27–7.20 (m, 1H), 7.19 (s, 1H), 3.79 (s, 3H). ^{13}C NMR ($CDCl_3$, 50 MHz): δ = 165.4, 156.2, 151.7, 149.2, 123.7, 122.5, 118.4, 61.2. Calcd. for $C_9H_8N_2OS$: 192.0357, HRMS *m*/*z*: 192.0349. Anal. calcd for $C_9H_8N_2OS$: C 56.23, H 4.19, N 14.57; found: C 56.38, H 4.23, N 14.36%.

5-Methoxy-2-(3-pyridyl)thiazole (3-MPT). Yield: 58%. Mp: 47–48 °C. IR (KBr, cm^{-1}): 1529, 1491, 1426, 1419, 1312, 1285, 1277, 1219, 961, 811. ^1H NMR ($CDCl_3$, 200 MHz): δ = 9.03–9.02 (m, 1H), 8.62–8.59 (m, 1H), 8.13–8.09 (m, 1H), 7.39–7.33 (m, 1H), 7.19 (s, 1H), 3.99 (s, 3H). ^{13}C-NMR ($CDCl_3$, 50 MHz): δ = 164.6, 150.1, 147.4, 144.4, 154.0, 131.4, 124.7, 122.8, 61.7. Calcd for $C_9H_8N_2OS$: 192.0357, HRMS (*m*/*z*): 192.0358. Anal. calcd for $C_9H_8N_2OS$: C 56.23, H 4.19, N 14.57; found: C 56.48, H 4.29, N 14.12%.

5-Methoxy-2-(4-pyridyl)thiazole (4-MPT). Yield: 50%. Mp: 56–57 °C. IR (KBr, cm^{-1}): 1595, 1525, 1494, 1458, 1419, 1313, 1286, 1276, 1221, 988, 830, 818, 800. ^1H NMR (CDCl3, 200 MHz): δ = 8.66 (d, J = 5.8 Hz, 2H), 7.69 (d, J = 5.8 Hz, 2H), 7.23 (s, 1H), 4.00 (s, 3H). ^{13}C NMR ($CDCl_3$, 50 MHz): δ = 164.9, 151.7, 150.1, 141.3, 123.0, 119.5, 61.6. Calcd for $C_9H_8N_2OS$: 192.0357, HRMS (*m*/*z*): 192.0358. Anal. calcd for $C_9H_8N_2OS$: C 56.23, H 4.19, N 14.57; found: C 56.40, H 3.91, N 14.28%.

Acknowledgements

The authors thank the NSFC (No. 20201009, 20221101, 20490210) for financial support.

References

1 (*a*) A. P. de Silva, H. Q. N. Gunaratne, T. Gunnlaugsson, A. J. M. Huxley, C. P. McCoy, J. T. Rademacher and T. E. Rice, *Chem. Rev.*, 1997, **97**, 1515; (*b*) J. Lin, *Trends Anal. Chem.*, 2000, **19**, 541; (*c*) J. A. Ferguson, B. G. Healey, K. S. Bronk, S. M. Barnard and D. R. Walt, *Anal. Chim. Acta*, 1997, **340**, 123.

2 (*a*) V. G. Young, H. L. Quiring and A. G. Sykes, *J. Am. Chem. Soc.*, 1997, **119**, 12477; (*b*) A. Safavi and H. Abdollahi, *Anal. Chim. Acta*, 1998, **367**, 167; (*c*) A. Lobnik, I. Oehme, I. Murkovic and O. S. Wolfbes, *Anal. Chim. Acta*, 1998, **367**, 159; (*d*) J. Lin and D. Liu, *Anal. Chim. Acta*, 2000, **408**, 49; (*e*) M. Cajlakovic, A. Lobnik and T. Werner, *Anal. Chim. Acta*, 2002, **455**, 207; (*f*) M. Elhabiri, O. Siri, A. Sornosa-Tent, A.-M. Albrecht-Gary and P. Braunstein, *Chem.–Eur. J.*, 2004, **10**, 134; (*g*) C.-G. Niu, G.-M. Zeng, L.-X. Chen, G.-L. Shen and R.-Q. Yu, *Analyst*, 2004, **129**, 20; (*h*) Z. Wang, Y. Xing, H. Shao, P. Lu and W. P. Weber, *Org. Lett.*, 2005, **7**, 87; (*i*) K. M.-C. Wong, W.-S. Tang, X.-X. Lu, N. Zhu and V. W.-W. Yam, *Inorg. Chem.*, 2005, **44**, 1492.

3 H. R. Kermis, Y. Kostov, P. Harms and G. Rao, *Biotechnol. Prog.*, 2002, **18**, 1047.

4 (*a*) *Molecular Fluorescence: Principles and Applications*, ed. B. Valeur, Wiley-VCH, Weinheim, 2002; (*b*) T. Gunnlaugsson, *Tetrahedron Lett.*, 2001, **42**, 8901; (*c*) G. T. Hanson, T. B. McAnaney, E. S. Park, M. E. P. Rendell, D. K. Yarbrough, S. Chu, L. Xi, S. G. Boxer, M. H. Monstrose and S. J. Remington, *Biochemistry*, 2002, **41**, 15477; (*d*) T. B. McAnaney, E. S. Park, G. T. Hanson, S. J. Remington and S. G. Boxer, *Biochemistry*, 2002, **41**, 15489; (*e*) T. Gunnlaugsson, J. P. Leonard, K. Sénéchal and A. J. Harte, *J. Am. Chem. Soc.*, 2003, **125**, 12062.

5 (*a*) S. Charier, O. Ruel, J.-B. Baudin, A. Alcor, J.-F. Allemand, A. Meglio and L. Jullien, *Angew. Chem., Int. Ed.*, 2004, **43**, 4785; (*b*) S. Charier, O. Ruel, J.-B. Baudin, D. Alcor, J.-F. Allemand, A. Meglio, L. Jullien and B. Valeur, *Chem.–Eur. J.*, 2006, **12**, 1097.

6 J. V. Metzger, *Thiazole and its Derivatives*, Wiley-Interscience, New York, 1979.

7 L. G. Lee, C. H. Chen and L. A. Chiu, *Cytometry*, 1986, **7**, 508.

8 V. M. Sonpatki, M. R. Herbert, L. M. Sandvoss and A. J. Seed, *J. Org. Chem.*, 2001, **66**, 7283.

9 W. R. Dawson and M. W. Windsor, *J. Phys. Chem.*, 1968, **72**, 3251.

10 O. Bossart, L. De Cola, S. Welter and G. Calzaferri, *Chem.–Eur. J.*, 2004, **10**, 5771.

11 (*a*) E. Lippert, *Z. Naturforsch., A: Astrophys. Phys. Phys. Chem.*, 1955, **10**, 541; (*b*) C. Reichardt, *Solvents and Solvent Effects in Organic Chemistry*, Wiley-VCH, Weinheim, 2003.

12 D. Laage, W. H. Thompson, M. Blanchard-Desce and J. T. Hynes, *J. Phys. Chem. A*, 2003, **107**, 6032.

13 (*a*) M. J. Frisch, G. W. Trucks, H. B. Schlegel, G. E. Scuseria, M. A. Robb, J. R. Cheeseman, J. A. Montgomery, Jr., T. Vreven, K. N. Kudin, J. C. Burant, J. M. Millam, S. S. Iyengar, J. Tomasi, V. Barone, B. Mennucci, M. Cossi, G. Scalmani, N. Rega, G. A. Petersson, H. Nakatsuji, M. Hada, M. Ehara, K. Toyota, R. Fukuda, J. Hasegawa, M. Ishida, T. Nakajima, Y. Honda, O. Kitao, H. Nakai, M. Klene, X. Li, J. E. Knox, H. P. Hratchian, J. B. Cross, V. Bakken, C. Adamo, J. Jaramillo, R. Gomperts, R. E. Stratmann, O. Yazyev, A. J. Austin, R. Cammi, C. Pomelli, J. Ochterski, P. Y. Ayala, K. Morokuma, G. A. Voth, P. Salvador, J. J. Dannenberg, V. G. Zakrzewski, S. Dapprich, A. D. Daniels, M. C. Strain, O. Farkas, D. K. Malick, A. D. Rabuck, K. Raghavachari, J. B. Foresman, J. V. Ortiz, Q. Cui, A. G. Baboul, S. Clifford, J. Cioslowski, B. B. Stefanov, G. Liu, A. Liashenko, P. Piskorz, I. Komaromi, R. L. Martin, D. J. Fox, T. Keith, M. A. Al-Laham, C. Y. Peng, A. Nanayakkara, M. Challacombe, P. M. W. Gill, B. G. Johnson, W. Chen, M. W. Wong, C. Gonzalez and J. A. Pople, *GAUSSIAN 03 (Revision B.05)*, Gaussian, Inc., Pittsburgh, PA, 2003; (*b*) P. J. Hay and W. R. Wadt, *J. Chem. Phys.*, 1985, **82**, 270; (*c*) P. J. Hay and W. R. Wadt, *J. Chem. Phys.*, 1985, **82**, 299; (*d*) W. R. Wadt and P. J. Hay, *J. Chem. Phys.*, 1985, **82**, 284; (*e*) C. Lee, W. Yang and R. G. Parr, *Phys. Rev. B*, 1988, **37**, 7.

14 For comparison, we also calculated the pK_a* values of 5-(4′-methoxyphenyl)-2-(pyridyl)oxazole (2- and 4-PYMPO) with eqn. (3) and found that our results (11.7 and 12.8 for 2- and 4-PYMPO, respectively) were in good agreement to the reported values (11.6 and 12.7 for 2- and 4-PYMPO, respectively) given in ref. 5*b*.

